Balancing Energy and Material Efficiency in Green Hydrogen Production via Water Electrolysis

Lejeune, Michaël; Daiyan, Rahman; Hauschild, Michael Zwicky; Kara, Sami

Published in:
Procedia CIRP

Link to article, DOI:
10.1016/j.procir.2024.01.130

Publication date:
2024

Document Version
Publisher's PDF, also known as Version of record

Available online at www.sciencedirect.com

ScienceDirect

Procedia CIRP 122 (2024) 958–963

www.elsevier.com/locate/procedia

31st CIRP Conference on Life Cycle Engineering (LCE 2024)

Balancing Energy and Material Efficiency in Green Hydrogen Production via Water Electrolysis

Michaël Lejeune[a,b], Rahman Daiyan[b,c,*], Michael Zwicky Hauschild[d], Sami Kara[a,b,*]

[a]*Sustainability in Manufacturing and Life Cycle Engineering Research Group, School of Mechanical and Manufacturing Engineering, The University of New South Wales, Sydney 2052, Australia*

[b]*Australian Research Council, Training Centre for the Global Hydrogen Economy, Sydney 2052, Australia*

[c]*School of Minerals and Energy Engineering, The University of New South Wales, Sydney 2052, Australia*

[d]*Division for Quantitative Sustainability Assessment (QSA), Department of Environmental and Resource Engineering, Technical University of Denmark, Kgs. Lyngby, Denmark*

* Corresponding author. *E-mail address:* s.kara@unsw.edu.au, r.daiyan@unsw.edu.au

Abstract

Green hydrogen is increasingly regarded as a pivotal solution in achieving “net zero by 2050” in carbon neutrality across various sectors and industries. Ambitious decarbonisation roadmaps largely depend on the successful deployment of electrolysis technologies. Among these, Proton Exchange Membrane Electrolysis (PEMEL) stands out for its efficiency, compact design, and adaptability to intermittent renewable power sources. PEMEL is gradually being commercialised, and considerable uncertainty remains regarding its future environmental performance at a plant level. Therefore, future PEMEL cells should be life cycle engineered with a focus on improving materials efficiency by investigating enhanced electrochemical catalysts, membranes, and electrodes for an improved membrane electrode assembly (MEA). In this study, we simulate a 10MW PEMEL plant, identify key operational parameters and evaluate future MEA development scenarios to assess their impact on energy consumption, material utilisation, and system durability. Our findings shed light on the potential trade-offs between energy and material efficiency, providing valuable insights to mitigate environmental hotspots. By focusing on these trade-offs, this work contributes significantly to the ongoing efforts to improve the environmental and operational performance of PEMEL plants.

Keywords: Life cycle engineering, Proton exchange membrane electrolysis, water electrolysis, Zero dimensional modelling

1. Introduction

Decarbonising major sectors and industries has become imperative to stay below 2°C of global warming. Current strategies heavily rely on hydrogen produced via water electrolysis as a low-emission energy carrier for the deep decarbonisation of hard-to-abate sectors and industries where direct electrification is a challenge [1].

Recent development scenarios from the International Energy Agency (IEA) estimate 3.3TW of global installed capacity for water electrolysis technologies, and 15000 TWh of electricity is required to reach net zero emission (NZE) by 2050 [2]. Among the key electrolysis technologies, proton exchange membrane electrolysis (PEMEL) is expected to provide nearly 40% of the green hydrogen market by 2050 [2]. While PEMEL technologies are increasingly being commercialised and deployed [2], there are still some uncertainties regarding their future environmental performance. This underlines the need for a comprehensive environmental assessment of PEMEL, not only to identify potential environmental hotspots but also life cycle engineering levers for mitigation strategies.

Hydrogen production via water electrolysis is widely known as an energy and water-intensive process with associated environmental stressors [3]. Depending on the energy source

10.1016/j.procir.2024.01.130

used in the process, the specific environmental impacts of hydrogen can be particularly high. This is because the source of energy embodies most of the environmental impacts. However, in a future-oriented analysis where renewable energy sources carry significantly less embodied impacts, the share of the impact of a PEMEL plant could reach up to 30% [4]. Hence, integrating life cycle engineering options in the research and development of PEMEL is crucial. This study focuses on the current and future development scenarios for PEMEL with an emphasis on energy consumption, material utilisation and system lifetime.

1.1. Challenge in proton exchange membrane electrolysis.

A definite advantage of PEMEL over other water electrolysis technologies is that it can operate at relatively high current densities of 1.5-3A/cm^2 (higher hydrogen production for a given active cell area) with an operating voltage ranging from 1.8-2.2V [5]. Other important aspects of PEMEL include high gas purity, negligible oxygen contamination in hydrogen, 30 to 35 bars hydrogen natural output pressure and fast response to change in current input, making PEMEL the most suitable technology for integration with renewable intermittent sources such as wind and solar energy [5]. A common PEMEL cell configuration (see Fig. 1) includes a proton-conducting perfluoro sulfonic polymer (Nafion® or Ryton®) that is coated with a catalyst layer (CL) on the anodic and cathodic sides. This is commonly called catalyst-coated membrane (CCM) or membrane electrode assembly (MEA).

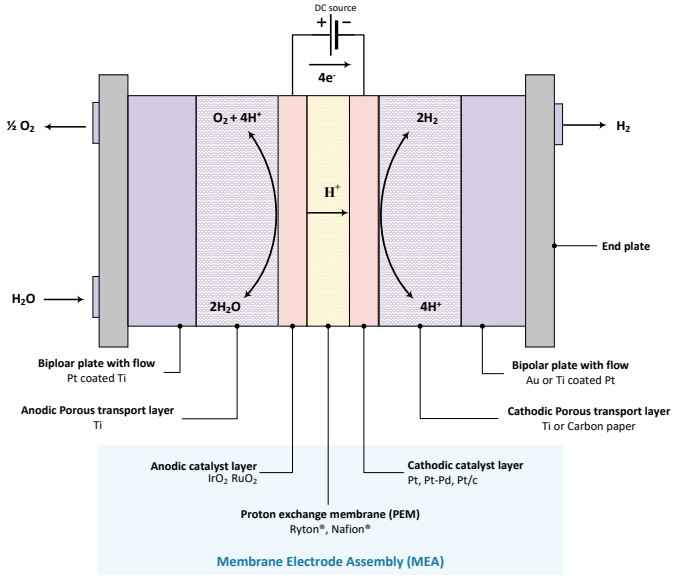

Fig. 1. Qualitative representation of a proton exchange membrane electrolysis cell.

Iridium oxide (IrO_2)- or ruthenium oxide (RuO_2)-based CL are commonly used for the oxygen evolution reaction (OER) where, as the name implies, oxygen is formed via oxidation. Platinum (Pt)-based CL, on the other hand, is used for the hydrogen evolution reaction (HER) where hydrogen is formed via reduction. The choice of IrO_2, RuO_2 and Pt as CLs has particular significance since they are the only known materials to sustain the harsh acidic environment of the cell while exhibiting a great catalytic performance. These materials have a significant influence on the reaction kinetics and, hence, on the performance of the cell. OER has much slower reaction kinetics than HER. Therefore, researchers primarily focus on improving the catalytic activity of OER. Apart from this, porous transport layers (PTLs) and bipolar plates (BPPs) with flow are necessary to transport fluids through the cell and electrons. Typically, these components are made of titanium (Ti) and coated with gold (Au) or Pt to avoid corrosion-induced passivation. Such passivation could lead to higher interfacial contact resistance and increased ohmic resistance through the cell.

Maintaining electrocatalytic performance while reducing the loadings of platinum group metals (PGMs) is a major research challenge for PEMEL [6]. This task is made more difficult by the limited global for Iridium (Ir), which currently stands at only 7 tonnes per year and is a major limiting factor for the rapid large-scale deployment of PEMEL [7]. To reduce the cost of hydrogen, research and development efforts are focused on decreasing the state-of-the-art Ir loadings (Ir-L), which currently ranges from 2-5mg/cm^2 to just 0.05mg/cm^2 [6]. Schropp *et al.* [4] recently investigated the environmental impacts of a PEMEL plant and found that when looking at the plant components, the global warming potential (GWP) of the electrolyser stack (i.e., an assembly of several electrolytic cells) is nearly three times higher than the balance of plant (BoP). The anode materials and BPP have the highest contributions because of the Ir, Pt and Ti loadings, which are environmentally intensive materials. The end plates and spraying of CLs on the membrane are also found to be significant contributors to the overall impacts. Surprisingly, the membrane is found to have a relatively small contribution to the GWP of the stack. As highlighted by Stropnik *et al.* [8], Nafion® is produced via the copolymerisation of tetrafluoroethylene and perfluoro (alkyl, vinyl ether) with sulfonyl acid fluoride, which is part of the perfluorocarbons and fluorocarbons. These chemicals have a significant GWP due to their long lifetime in the atmosphere, which can span thousands of years [8]. Furthermore, Nafion® shows excellent proton conductivity but is an electron insulator. Due to its lower conductivity compared to PTL, BPP, and CL components, the thickness of the membrane plays a crucial role in the MEA cell performance [9].

Building on these considerations and mitigation strategies defined by Kara *et al.* [10], some life cycle engineering levers can be identified at the manufacturing and operation stage:

i. Improving the OER catalytic performance with reduced Ir loadings in MEA.
ii. Reducing membrane thickness.
iii. Reducing BPP and PTL thickness.
iv. Use of low-emission electricity.

The energy consumption in the water electrolysis process is directly influenced by various factors, including electrode geometry, cell design, microfluidic plates, and cell materials. This study aims to implement these life cycle engineering levers based on future MEA scenarios using a zero-dimensional PEMEL model to evaluate potential emission savings.

2. Methodology

2.1. Electrochemical model

The cell voltage U_{cell} and current density j are essential parameters to measure the performance of electrolysis-based systems. While the current density is simply the rate of electric charge passing through a unit of surface area of electrodes (i.e., A/cm^2), the cell voltage depends on the current density applied to the cell. U_{cell} is composed of the reversible voltage U_{rev} and the sum of overpotentials (Eqn.1). In this equation, U_{rev} was determined using the pressure and temperature dependent Nernst equation [11].

$$U_{cell} = U_{rev} + \hat{\eta}_{act} + \hat{\eta}_{ohm} + \hat{\eta}_{diff} + \hat{\eta}_{degrad} \quad (1)$$

$\hat{\eta}_{act}$ refers to the activation overpotential, which is driven by reaction kinetics. This term can be derived directly from the Butler-Volmer equation [12] or the simplified Tafel equation [12,13]. In this study, $\hat{\eta}_{act}$ is derived and adapted from the Butler-Volmer equation and account for the intrinsic catalytic activity of Iridium $j_{0,Ir}$ based on the Ir loading L_{Ir} (see Eqn.2). Where R is the ideal gas constant, T is the operating temperature, and α_{an} , the electron transfer coefficient on the anodic side was set to 0.5 [12].

$$\hat{\eta}_{act} = \frac{RT}{\alpha_{an}F}\sinh^{-1}\left(\frac{j}{2j_{0,Ir}L_{Ir}}\right) \quad (2)$$

The electrical resistance of the cell can contribute significantly to the cell overpotential at high current densities. Building on this, the ohmic overpotential $\hat{\eta}_{ohm}$ is represented by Eqn.3. It is primarily driven by the conductivities and geometries of the membrane, BPP, and PTL. To reduce modelling complexity, the total thickness at the anode and cathode, noted δ_{an} and δ_{cat}, include the BPP, PTL and CL. A uniform resistivity is assumed on both sides, noted ρ_{an} and ρ_{cat}. The electrode thickness is 1.3mm and resistivity 7.5mΩcm for both the anode and cathode [13]. The membrane conductivity σ_{mem} was derived using the model from Springer *et al.* [14] the membrane thickness δ_{mem} is variable in this study.

$$\hat{\eta}_{ohm} = j\left(\delta_{an}\rho_{an} + \delta_{cat}\rho_{cat} + {}^{\delta_{mem}}/_{\sigma_{mem}}\right) \quad (3)$$

At high current densities, the reaction is mainly driven by mass transfer rather than electron transfer [12]. To capture mass transfer limitations due to concentration gradient, the diffusion (concentration) overpotential $\hat{\eta}_{diff}$ is defined. It can be modelled by imposing a limiting current density j_L as in Eqn.4 or using concentrations gradients [12]. The former formulation was employed with an assumed limiting current density of 6A/cm^2.

$$\hat{\eta}_{diff} = \frac{RT}{\alpha_{an}nF}\ln\left(\frac{j_L}{j_L - j}\right) \quad (4)$$

Lastly, the cell is unlikely to preserve its performance over time. For this reason, a time-dependent degradation overpotential $\hat{\eta}_{degrad}(t)$ is introduced and described by Eqn.5. In this equation, γ_i and t are the degradation rate for i components and the time in hours, respectively. The degradation rate for the MEA γ_{MEA} and PLT are assumed to be 3µV/h and γ_{PLT} 12µV/h, respectively.

$$\hat{\eta}_{degrad}(t) = \sum_i \gamma_i \times t \quad (5)$$

The electrochemical model has been validated using extrapolated polarisation curve data from Crespi *et al.* [15] and using their operating parameters.

2.2. Plant mass transport and energy balance

Mass transport in the cell was rigorously modelled based on models provided by refs [15,16]. At a plant level, the Aspen plus analyser was used to retrieve vapour liquid equilibrium data based on the NRTL activity coefficient model for binary mixtures. The overall plant mass and energy balance model was built on Python using the Cantera package as thermodynamic engine. BoP components were modelled using high-level heuristics methods. To operate at constant temperature, the plant control strategy focused on the stacks' inlet water temperature. The plant configuration is provided in Fig. 2. Further information on the PEMEL generic plant configuration is provided by Crespi *et al.* [15].

2.3. Material and energy efficiencies

Materials in the electrolysis have a significant contribution to GWP, hence, reducing or finding an optimal balance with energy consumption is of the essence. However, defining the material efficiency is not as straightforward due to the variety of materials used in a PEMEL cell. Because Ir loading and its catalytic activity are one of the prime issues to be tackled for the MEA development, it is assumed that the material efficiency η_{Ir} is a ratio of Iridium-specific power density $P_{d,Ir}$ and the target value by 2050 which is assumed to be 0.04mg/W [7] (Eqn.6).

$$\eta_{Ir} = \frac{P_{d,Ir}^{2050}}{P_{d,Ir}} = \frac{P_{d,Ir}^{2050}}{L_{Ir}} jU_{cell} \quad (6)$$

The energy efficiency η_{energy} at a plant level is based on the lower heating value of hydrogen LHV and the plant-specific energy consumption SEC is defined in Eqn.7.

$$\eta_{energy} = \frac{LHV}{SEC} \quad (7)$$

The cell lifetime is assumed to be dependent on L_{Ir}, the dissolution rate ζ and the load factor LF as in Eqn.8 [7].

$$lifetime = \frac{L_{Ir}}{LF \times \zeta} = \frac{P_{cell,rated}\, L_{Ir}}{P_{cell} \times \zeta} \quad (8)$$

To capture a variation in the lifetime as a function of the operating current density, the load factor *LF* was defined as the ratio of the operating cell power P_{cell} against the rated cell power $P_{cell,rated}$. As cells are electrically connected in series in a PEMEL stack, it is a reasonable assumption to limit the lifetime at a cell level.

2.4. Life cycle performance

An attributional life cycle assessment (LCA) was conducted to evaluate the environmental performance of PEMEL with future MEA scenarios using a cradle-to-gate approach. The functional unit was defined as a kilogram of dry hydrogen produced at 30 bars pressure and 65°C with 99.9% purity. The LCA was carried out using the *Brightway2* Python package, and background data is sourced from Ecoinvent v3.9.1 "*allocation cut-off by classification*". The plant inventory was adapted from ßareiss *et al.* [17] and Delpierre *et al.* [18]. To determine the mass of Ir, membrane, and Pt, the geometry of materials and their densities were used and parameterised using the *lca_algebraic* v10.0 Python package. The focus of this study is to evaluate the global warming potential (GWP) over 100 years, and the IPCC 2021 method was selected accordingly.

2.5. Case study: 10MW electrolysis plant

The reference scenario involves a 10MW electrolyser plant, (see Fig. 2) operating continuously for 80000 hours under steady-state conditions. It is assumed to be powered by wind electricity, and that the load factor depends on the operating current density. This factor is assumed to remain constant throughout the project's lifetime at the specific operating current density. By doing so, it is possible to make the environmental assessment dependent on the operating conditions. The plant operating parameters are listed in Table 2. To account for the change in performance at both the cell and plant levels, optimistic development scenarios were obtained from Clapp *et al.* [7] (see Table 1).

Table 1. Current and future value for key MEA components based on ref [7].

MEA parameters	Reference	2030	2050
L_{Ir} (mg_{Ir}/cm^2)	1.89	0.27	0.1
$j_{0,Ir}$ $\times 10^{-7}$ (A/mg_{Ir})	1.5	10	27
δ_{mem} (µm)	125	80	50
ζ $\times 10^{-6}$ ($mg_{Ir}/cm^2/h$)	12	8	2.0

3. Results and discussion

3.1. Current and future performance

Fig. 3 shows the influence of the catalytic activity of Ir and operating current density on the cell efficiency based on the lower heating value (LHV) of hydrogen with fixed membrane thickness and Ir loadings based on the base case scenario. With faster reaction kinetics at the anode (i.e., higher $j_{0,Ir}$), the cell efficiency increases accordingly. At a fixed current density, e.g., 2A/cm², the efficiency gain is 3% with 2050 $j_{0,Ir}$ values. It can also be observed that operating at higher current densities comes at the expense of energy efficiency. For instance, a drop in efficiency of 4% is found when switching from 2 to 3A/cm² for both the reference and 2050 scenarios.

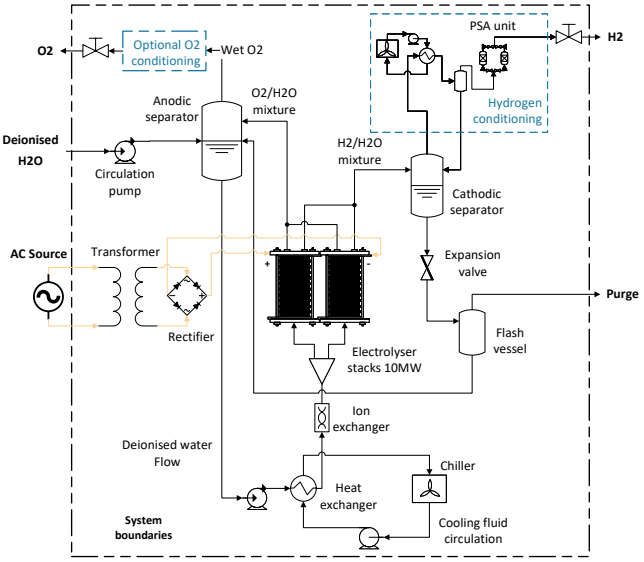

Fig. 2. 10MW PEM electrolysis plant configuration composed of two 5MW electrolyser stacks electrically connected in parallel.

Table 2. Water electrolysis plant reference parameters

Parameter	Value	Source
Number of stacks	2	Constant
Plant rated power (MW)	10	Constant
Operating current density (A/cm^2)	2	Constant
Cell voltage at current density (V)	1.90	Calculated
Operating temperature ($°C$)	65	Constant
Cathode operating pressure (bar)	30	Constant
Anode operating pressure (bar)	1.6	Constant
Number of cells	2534	Calibrated
Active cell area (cm^2)	500	Assumed

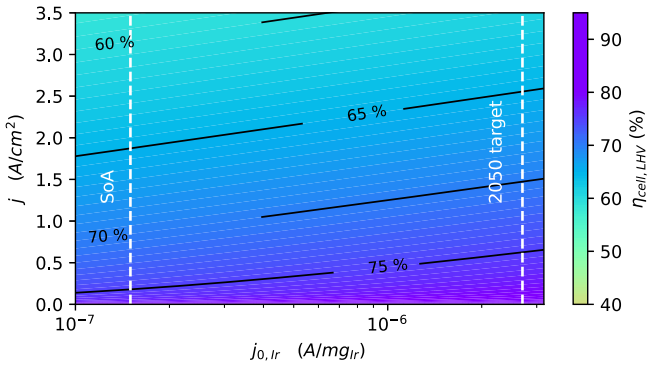

Fig. 3. Representation of the cell efficiency based on the lower heating value of hydrogen as a function of the catalytic activity and the operating current density with fixed iridium loading and membrane thickness. The dashed white represents the state-of-the-art (SoA) value for the catalytic activity and the target value by 2050.

The efficiency improvement is more significant in the activation region, i.e., at low current densities below 0.5A/cm^2. This analysis was performed using a constant iridium loading. It is important to note that based on our model, reducing the Iridium loading would decrease cell performance if the catalytic activity remains the same.

The influence of the membrane thickness on the cell efficiency with fixed Ir loading and catalytic activity is shown in Fig. 4. At low current density, in the activation region, the cell resistance reaches a constant value, with no efficiency improvement for future scenarios. This rapidly changes when operating at current densities higher than 0.5A/cm^2, i.e., frontier to ohmic region. When comparing the reference and 2050 scenarios, it can be observed that at 2A/cm^2, the gain in efficiency is 4%. At 3A/cm^2, the gain in efficiency is even higher, with 6%. However, the loss in efficiency when switching from 2 to 3A/cm^2 scenario is 4% at 125µm and 2% at 50µm.

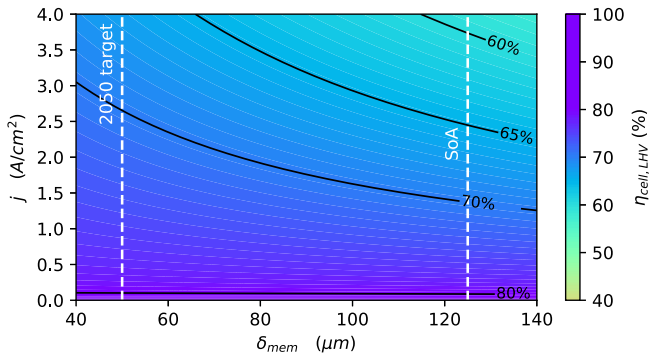

Fig. 4. Evolution of the cell efficiency as a function of the membrane thickness and current density at fixed Iridium loading and activity.

At a plant level, the future improvements are clearly visible in Fig. 5 where the specific energy consumption (SEC) of the plant is shown as a function of the operating current density. In the reference scenario, the SEC of the plant is 55.44kWh/kgH_2, which is similar to the value reported by the US Department of Energy (DoE) [19]. However, for future scenarios the DoE potentially assumes a higher operating temperature than that of this study which is one of the likely reasons for this discrepancy. The reference scenario shows a significant decrease in energy consumption for future scenarios. The stacks are responsible for 51.55kWh/kgH_2, while the BoP contributes 3.90kWh/kgH2. The plant's overall efficiency, calculated using the LHV, is 58.9%. However, in the 2030 and 2050 scenarios, the plant efficiency is projected to increase to 61.2% and 63%, respectively. This translates to a SEC of 53.30kWh/kgH_2 and 51.8kWh/kgH_2 for the 2030 and 2050 scenarios, respectively.

3.2. Environmental performance

Water electrolysis is an energy-intensive process and reducing specific energy consumption (SEC) can lead to a proportional reduction in the global warming potential (GWP). Fig. 6 exemplifies this reduction in GWP when a wind-powered plant is operated. It is important to note that the operating current density remains constant throughout the entire lifespan of the plant, which is assumed to be 80000 hours. An interesting result of this study is that the operating current density is a lever to achieve a minimum GWP. The minimum GWP is reached when hydrogen production sufficiently distributes plant-embodied emissions at the specific current density. Implementing future MEA scenarios allows for a global reduction in GWP from 0.90kgCO_2eq/kgH_2 at 1.13A/cm^2 for the reference scenario to 0.85 and 0.83kgCO_2eq/kgH_2 and at 0.93 and 1A/cm^2 for the 2030 and 2050 scenarios, respectively. The production of hydrogen and the plant's energy efficiency are the main factors that contribute to GWP beyond these minimums. These findings contradict the technoeconomic approach of maximising hydrogen production by operating at high current densities throughout the plant's lifetime. This means the plant's environmental breakeven point is achieved at lower operating current densities (below 2A/cm^2), as opposed to the targets set by the DoE (3A/cm^2). Beyond this breakeven point, the GWP impact, while remaining low, gradually increases. It is important to mention that for electricity sourced from the electrical grid with a high emission factor (e.g., 15kgCO_2eq/kgH_2 for the European grid average according to the ecoinvent 3.9.1 database), no minimum GWP can be observed as it is eclipsed by the electricity embodied emissions which are significantly higher. This suggests that the trade-off between high hydrogen production and GWP exists for low-emission energy sources only. This supports the findings from Schropp *et al.* [4], as their work showed that the electrolysis plant's share of the total environmental impact is relatively higher when low-emission energy sources are used. To further contextualise results, the low hydrogen taxonomy set by the European Union was added as reference (i.e., <3kgCO_2eq/kgH_2). It can be interpreted that wind-based electrolysis can be operated at high current densities while remaining within the low-emission hydrogen margin.

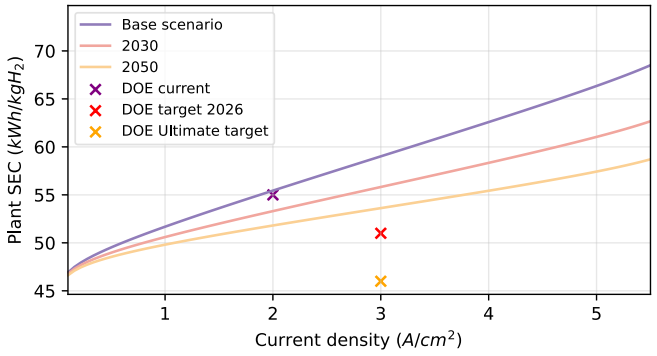

Fig. 5. Plant-specific energy consumption as a function of the operating current density, based on the simulated model. Data points refer to the current status of future targets for plant-specific energy consumption according to the US Department of Energy (DOE) [19]

Lastly, Fig. 7 shows the trade-offs between energy, material efficiencies and lifetime of the electrolysis plant. It should be noted that results are reduced to a meaningful feasibility region as the lifetime and material efficiency are inversely proportional. The results indicate a region where the GWP is the lowest at high energy efficiency and low reduction in lifetime. This is because, at low current density, there is only a small reduction in lifetime, and high energy efficiency and low power input enable the lower GWP values. Contrastingly, high material efficiency is achieved at high current densities.

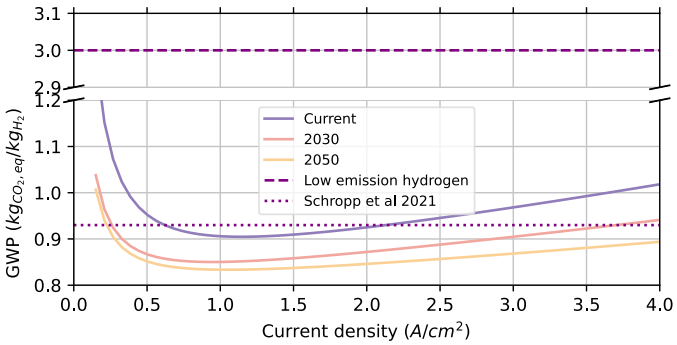

Fig. 6. Evolution of global warming potential as a function of the operating current density when the input power is from wind energy. The purple dashed line is the value found by Schropp *et al* [4], and the purple dotted line is the European standard threshold to define low-emission hydrogen.

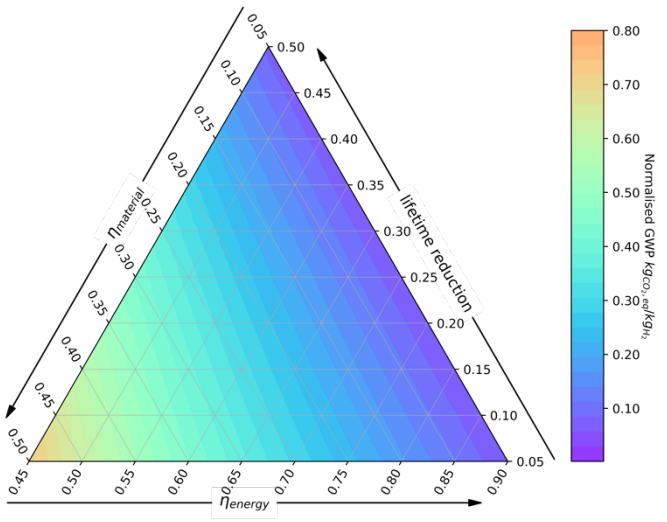

Fig. 7. The relationship between energy, material, lifetime reduction with global warming potential based on wind electricity. All values are normalised and restricted to a meaningful feasibility region. To interpret this figure, the reader should identify the ticks' orientation for a given axis.

With higher hydrogen production rates, the hydrogen output carries more emissions and translates to higher GWP values (see Fig. 6). Hence, favouring energy efficiency seems to be more beneficial from an environmental point of view.

4. Conclusion

This study explored the life cycle engineering levers for PEMEL through a zero-dimensional PEMEL model. The results show that the operating current density is the most important parameter for reducing GWP emissions. Trade-offs between conflicting trends, such as material and energy efficiencies and system lifetime, have also been examined. The study introduced an environmental dimension which provides valuable insights into these trade-offs. Our findings suggest that reducing the thickness of the membrane and increasing the catalytic activity of the iridium can help reduce GWP by improving energy consumption. Additionally, it is recommended to carefully choose the operating current density when using low-emission electricity to achieve greater emission reductions. Future work can extend the present study by implementing a complete life cycle engineering framework considering all life cycle stages and other environmental impact categories, such as water and resource depletion to further improve PEMEL environmental performance.

Acknowledgements

This work was supported by the Australian Research Council (ARC) Training Centre for The Global Hydrogen Economy (IC200100023).

References

[1] Amal, R., Daiyan, R., Polepalle, K., Khan, M. H., and Gao, T., 2021, *NSW Power to X (P2X) Pre-Feasibility Study*, UNSW, Sydney, Australia.
[2] IEA, 2021, *Net Zero by 2050 - A Roadmap for the Global Energy Sector*, IEA, Paris.
[3] Bhandari, R., Trudewind, C. A., and Zapp, P., 2014, "Life Cycle Assessment of Hydrogen Production via Electrolysis – a Review," J. Clean. Prod., **85**, pp. 151–163.
[4] Schropp, E., Naumann, G., and Gaderer, M., 2021, "Life Cycle Assessment of a Polymer Electrolyte Membrane Water Electrolysis," *Progress in Life Cycle Assessment 2019*, S. Albrecht, M. Fischer, P. Leistner, and L. Schebek, eds., Springer International Publishing, Cham, pp. 53–66.
[5] Buttler, A., and Spliethoff, H., 2018, "Current Status of Water Electrolysis for Energy Storage, Grid Balancing and Sector Coupling via Power-to-Gas and Power-to-Liquids: A Review," Renew. Sustain. Energy Rev., **82**, pp. 2440–2454.
[6] Chatenet, M., Pollet, B. G., Dekel, D. R., Dionigi, F., Deseure, J., Millet, P., Braatz, R. D., Bazant, M. Z., Eikerling, M., Staffell, I., Balcombe, P., Shao-Horn, Y., and Schäfer, H., 2022, "Water Electrolysis: From Textbook Knowledge to the Latest Scientific Strategies and Industrial Developments," Chem. Soc. Rev., **51**(11), pp. 4583–4762.
[7] Clapp, M., Zalitis, C. M., and Ryan, M., 2023, "Perspectives on Current and Future Iridium Demand and Iridium Oxide Catalysts for PEM Water Electrolysis," Catal. Today, **420**, p. 114140.
[8] Stropnik, R., Lotrič, A., Bernad Montenegro, A., Sekavčnik, M., and Mori, M., 2019, "Critical Materials in PEMFC Systems and a LCA Analysis for the Potential Reduction of Environmental Impacts with EoL Strategies," Energy Sci. Eng., **7**(6), pp. 2519–2539.
[9] Wrubel, J. A., Milleville, C., Klein, E., Zack, J., Park, A. M., and Bender, G., 2022, "Estimating the Energy Requirement for Hydrogen Production in Proton Exchange Membrane Electrolysis Cells Using Rapid Operando Hydrogen Crossover Analysis," Int. J. Hydrog. Energy, **47**(66), pp. 28244–28253.
[10] Kara, S., Herrmann, C., and Hauschild, M., 2023, "Operationalization of Life Cycle Engineering," Resour. Conserv. Recycl., **190**, p. 106836.
[11] Lamy, C., and Millet, P., 2020, "A Critical Review on the Definitions Used to Calculate the Energy Efficiency Coefficients of Water Electrolysis Cells Working under near Ambient Temperature Conditions," J. Power Sources, **447**, p. 227350.
[12] Olivier, P., Bourasseau, C., and Bouamama, Pr. B., 2017, "Low-Temperature Electrolysis System Modelling: A Review," Renew. Sustain. Energy Rev., **78**, pp. 280–300.
[13] Colbertaldo, P., Gómez Aláez, S. L., and Campanari, S., 2017, "Zero-Dimensional Dynamic Modeling of PEM Electrolyzers," Energy Procedia, **142**, pp. 1468–1473.
[14] Springer, T. E., Zawodzinski, T. A., and Gottesfeld, S., 1991, "Polymer Electrolyte Fuel Cell Model," J. Electrochem. Soc., **138**(8), pp. 2334–2342.
[15] Crespi, E., Guandalini, G., Mastropasqua, L., Campanari, S., and Brouwer, J., 2023, "Experimental and Theoretical Evaluation of a 60 kW PEM Electrolysis System for Flexible Dynamic Operation," Energy Convers. Manag., **277**, p. 116622.
[16] Abdin, Z., Webb, C. J., and Gray, E. MacA., 2015, "Modelling and Simulation of a Proton Exchange Membrane (PEM) Electrolyser Cell," Int. J. Hydrog. Energy, **40**(39), pp. 13243–13257.
[17] Bareiß, K., de la Rua, C., Möckl, M., and Hamacher, T., 2019, "Life Cycle Assessment of Hydrogen from Proton Exchange Membrane Water Electrolysis in Future Energy Systems," Appl. Energy, **237**, pp. 862–872.
[18] Delpierre, M., 2019, *An Ex-Ante LCA Study on Wind-Based Hydrogen Production in the Netherlands*, Leiden University, Leiden.
[19] DOE, 2023, "Technical Targets for Proton Exchange Membrane Electrolysis," Energy.gov [Online]. Available: https://www.energy.gov/eere/fuelcells/technical-targets-proton-exchange-membrane-electrolysis. [Accessed: 13-Nov-2023].